Revealing the catalytic potential of an acyl-ACP desaturase: Tandem selective oxidation of saturated fatty acids

Edward J. Whittle*, Amy E. Tremblay†, Peter H. Buist,† and John Shanklin*‡

*Department of Biology, Brookhaven National Laboratory, 50 Bell Avenue, Upton, NY 11973; and †Department of Chemistry, Carleton University, 1125 Colonel By Drive, Ottawa, ON, Canada K1S 5B6

Edited by Wendell Roelofs, Cornell University, Geneva, NY, and approved July 14, 2008 (received for review June 10, 2008)

It is estimated that plants contain thousands of fatty acid structures, many of which arise by the action of membrane-bound desaturases and desaturase-like enzymes. The details of ''unusual'' e.g., hydroxyl or conjugated, fatty acid formation remain elusive, because these enzymes await structural characterization. However, soluble plant acyl-ACP (acyl carrier protein) desaturases have been studied in far greater detail but typically only catalyze desaturation (dehydrogenation) reactions. We describe a mutant of the castor acyl-ACP desaturase (T117R/G188L/D280K) that converts stearoyl-ACP into the allylic alcohol *trans*-isomer (*E*)-10-18:1-9-OH via a cis isomer (*Z*)-9-18:1 intermediate. The use of regiospecifically deuterated substrates shows that the conversion of (*Z*)-9-18:1 substrate to (*E*)-10-18:1-9-OH product proceeds via hydrogen abstraction at C-11 and highly regioselective hydroxylation (>97%) at C-9. ^{18}O-labeling studies show that the hydroxyl oxygen in the reaction product is exclusively derived from molecular oxygen. The mutant enzyme converts (*E*)-9-18:1-ACP into two major products, (*Z*)-10-18:1-9-OH and the conjugated linolenic acid isomer, (*E*)-9-(*Z*)-11-18:2. The observed product profiles can be rationalized by differences in substrate binding as dictated by the curvature of substrate channel at the active site. That three amino acid substitutions, remote from the diiron active site, expand the range of reaction outcomes to mimic some of those associated with the membrane-bound desaturase family underscores the latent potential of O_2-dependent nonheme diiron enzymes to mediate a diversity of functionalization chemistry. In summary, this study contributes detailed mechanistic insights into factors that govern the highly selective production of unusual fatty acids.

binuclear iron | diiron | hydroxylation | nonheme iron | catalysis

It has been estimated that the seeds of plants contain thousands of structurally distinct fatty acids (1). Many fatty acid modification reactions are initiated by hydrogen removal from an unactivated methylene/vinyl group and result in oxidation of substrate (2). In all reactions described to date, an activated oxygen species formed at a diiron center (3, 4) is believed to effect the initial hydrogen abstraction. The recognition of this common initial step in fatty acid modification led Somerville and coworkers (5) to identify the gene encoding the oleoyl 12-hydroxylase based on its homology to the oleoyl 12-desaturase. Appreciation of the catalytic diversity of desaturase-like enzymes (6) stimulated a search for, and subsequent identification of, an acetylenase, epoxygenase (7), and enzymes responsible for the synthesis of conjugated fatty acids (8) and allylic alcohols (9). Progress toward understanding the determinants of reaction outcome has been achieved via comparative studies on the oleate-desaturase/hydroxylase pair involving systematic site-directed mutagenesis of residues proximal to the putative active site (10, 11). Unfortunately, further interpretation of these data will not be possible until this class of membrane-bound enzymes is structurally characterized.

Several crystal structures (12–15) are available for the structurally distinct, soluble acyl-acyl carrier protein (ACP) desaturases (6, 16–18) but this class of enzyme acts only as a desaturase with natural substrates and precludes the desired correlation of structure with a range of reaction outcomes. The acyl-ACP family of desaturases contains a number of members with different substrate chain length specificities and regioselectivities (6, 19). However, the absence of reported oxygenation chemistry compared with their membrane-bound counterparts is striking. In the present work, we describe a triple mutant of the castor desaturase that is able to convert stearoyl- or oleoyl-ACP to the allylic alcohol (*E*)-10-18:1-9-OH with high regioselectivity; the (*E*)-isomer of oleoyl-ACP, elaidyl-ACP, is converted to a mixture of (*Z*)-10-18:1-9-OH and the conjugated 9-(*E*)-11-(*Z*) isomer of linoleic acid (CLA). The different reaction outcomes are rationalized by distinct substrate binding modes in a curved active site.

Results and Discussion

Mutant Desaturase Converts Stearoyl Substrate to a Hydroxylated Product. During the course of experiments designed to understand the factors governing regioselectivity, we engineered a triple mutant T117R/G188L/D280K of the castor Δ9 desaturase (Fig. 1) (referred to in this article as ''mutant desaturase'') in an attempt to mimic structural features of the ivy Δ4 desaturase (14). The expected change in regioselectivity from Δ9 to Δ4 was not observed; however, the 18:0 substrate was converted into (*Z*)-9-18:1 product, which initially accumulated and then disappeared, as indicated by GC analysis (Fig. 2 *A–C*). The apparent mass balance deficit was restored upon derivatization of the product mixture with (*N,O-bis*[Trimethylsily]trifluoroacetamide) plus trimethylchlorosilane, whereupon a ~9:1 mixture of two new products (Fig. 2*D*) was observed. This result suggested that these novel products were alcohols. The mass spectra of the trimethylsilyl (TMS) derivatives of the major and minor hydroxylated product (Fig. 2 *E* and *F*) were indistinguishable from each other and featured an apparent molecular ion (*m/z* = 384) consistent with a C18 product containing an O-TMS group and a double bond. The presence of an *m/z* 227 ion in these mass spectra is diagnostic for an O-TMS group at C-9 and a double bond between C-9 and the methyl group of the fatty acid. The initial formation of (*Z*)-9-18:1-ACP, and its subsequent decrease in abundance with hydroxy product accumulation indicated that (*Z*)-9-18:1-ACP was a substrate for the mutant enzyme. This interpretation was confirmed by the observation of hydroxylated

Author contributions: J.S. designed research; E.J.W., A.E.T., and J.S. performed research; A.E.T. and P.H.B. contributed new reagents/analytic tools; E.J.W., A.E.T., P.H.B., and J.S. analyzed data; and P.H.B. and J.S. wrote the paper.

The authors declare no conflict of interest.

This article is a PNAS Direct Submission.

‡To whom correspondence should be addressed. E-mail: shanklin@bnl.gov.

This article contains supporting information online at www.pnas.org/cgi/content/full/0805645105/DCSupplemental.

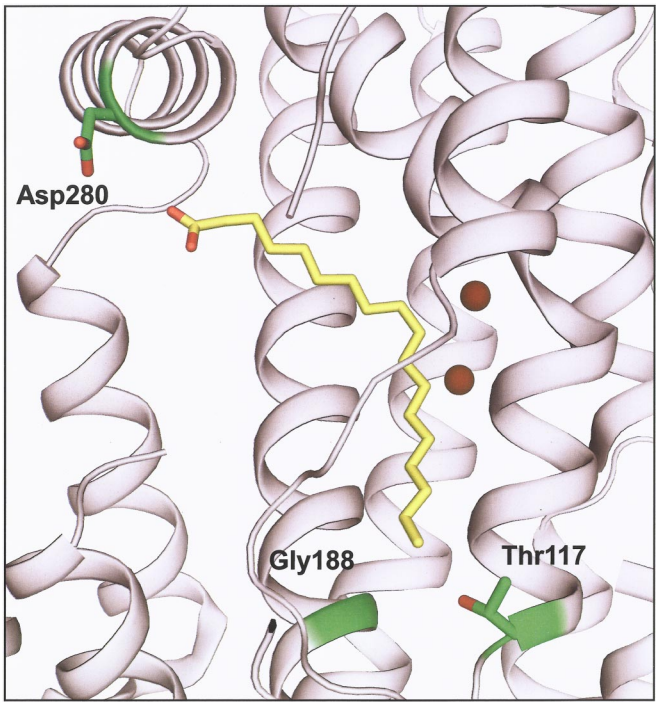

Fig. 1. Location of residues T117, G188, and D280 in the WT desaturase. The active site iron ions are shown as brown spheres; a model of the 18:0 substrate is shown in yellow.

product formation upon incubating (*Z*)-9-18:1-ACP with the mutant desaturase; the ratio of the two hydroxy components mimicked that obtained previously with 18:0-ACP substrate (Fig. 3*A*).

H-Abstraction from C-11 of Oleoyl Substrate Leads to the Highly Regioselective Formation of the 10-18:1-9OH Allylic Alcohol. The position of hydrogen abstraction in oleyl ACP oxidation was

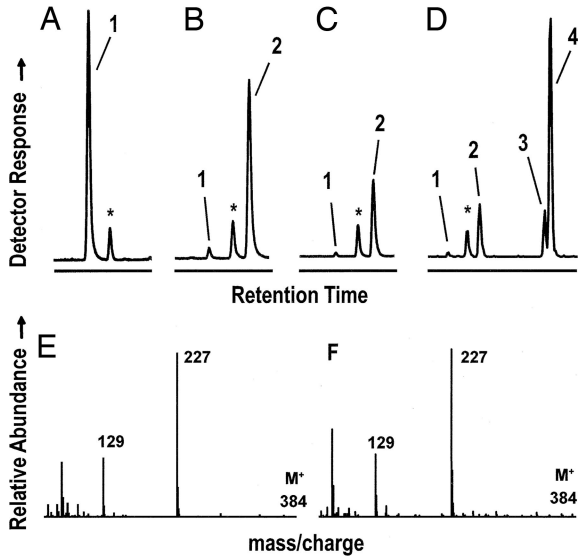

Fig. 2. Mutant desaturase converts 18:0-ACP into a pair of novel hydroxy monoenes. (*A–D*) Gas chromatographic separation of FAMES obtained from reaction mixtures at reaction time t = 0 (*A*), t = 0.5 h (*B*), and t = 5 h (*C* and *D*). *C* and *D* display chromatograms obtained before and after TMS derivatization, respectively. Fatty acid methyl esters: 1, 18:0; 2, (*Z*)-9-18:1; 3, minor product peak; 4, major product peak, *contaminant. (*E* and *F*) Mass spectra correspond to the peaks labeled 3 and 4, respectively.

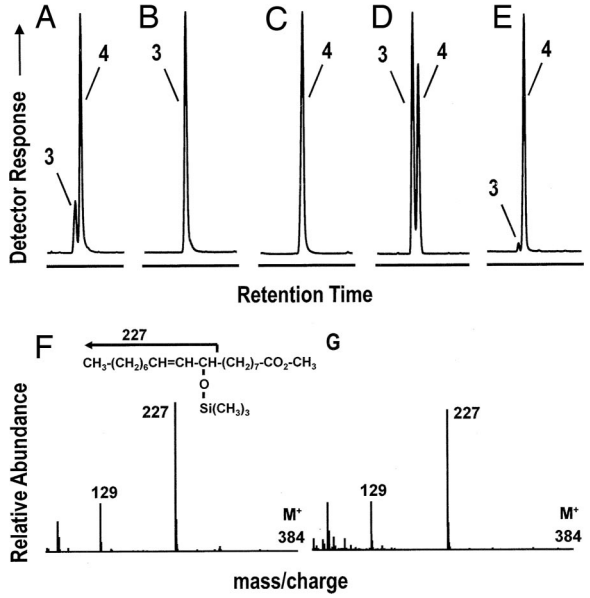

Fig. 3. Mutant desaturase product peaks are identified as (*Z*)- and (*E*)-isomers of the 10-18:1-9-OH allylic alcohol. Gas chromatographic separation of methyl esters following TMS derivatization displays the conversion of (*Z*)-9-18:1-ACP substrate to product (*A*), synthetic (*Z*)-10-18:1-9-OH standard (*B*), synthetic (*E*)-10-18:1-9-OH standard (*C*), combination of samples *A* and *B* (*D*), and combination of samples *A* and *C* (*E*). Numbers on the gas chromatograms have the same designation as in Fig. 2. (*F* and *G*) Mass spectra corresponding to the synthetic standard (*Z*)-10-18:1-9-OH in *B* and corresponding to the synthetic standard (*E*)-10-18:1-9-OH in *C*, respectively, are shown.

identified by incubating dideuterated acyl-ACPs with the mutant desaturase and mass spectral analysis of the hydroxyl products (Table 1). The 9,10-d_2-oleyl- (Cambridge Isotope Labs) and 11d_2-oleyl-ACPs (20) were prepared from available labeled oleic acid precursors, but 12d_2-oleyl-ACP was generated *in situ* from 12-d_2-stearoyl-ACP (20). Gas chromatography-mass spectrometry analysis of the products obtained from these incubations revealed that one deuterium was removed when 11-d_2-oleoyl-ACP was presented as substrate, whereas both deuterium atoms were retained in the product when the label was present at C-9, C-10, or C-12. Consideration of these results, together with the mass spectral data discussed previously, led us to propose an allylic alcohol structure, namely (*Z*)- or (*E*)-10-18:1-9-OH for the novel hydroxyl products obtained from this mutant desaturase. To confirm the position of the hydroxyl group and to assign the stereochemistry of the double bond in this product mixture, we synthesized four standards [(*Z*)- and (*E*)-10-18:1-9-OH, (*Z*)- and (*E*)-9-18:1-11-OH) using standard synthetic routes [see the supporting information (SI)]. A comparison of the mass spectra

Table 1. Mass Spectral data for 10-18:1-9-OH, TMS derivative obtained from incubation of various deuterated substrates with mutant desaturase

Substrate	Molecular ion	Major* fragment ion of 10-18:1-9-OTMS
d0 stearate	384†	227‡
d0 oleate	384	227
9,10d2 oleate	386	229
11d2 oleate	385	228
12d2 stearate	386	229

*Fragment represents >95% of the total ion current.
†Molecular ion of product (10-18:1-9-OTMS) methyl ester.
‡Mass of fragment ion due to cleavage between carbons 8 and 9.

PLANT BIOLOGY

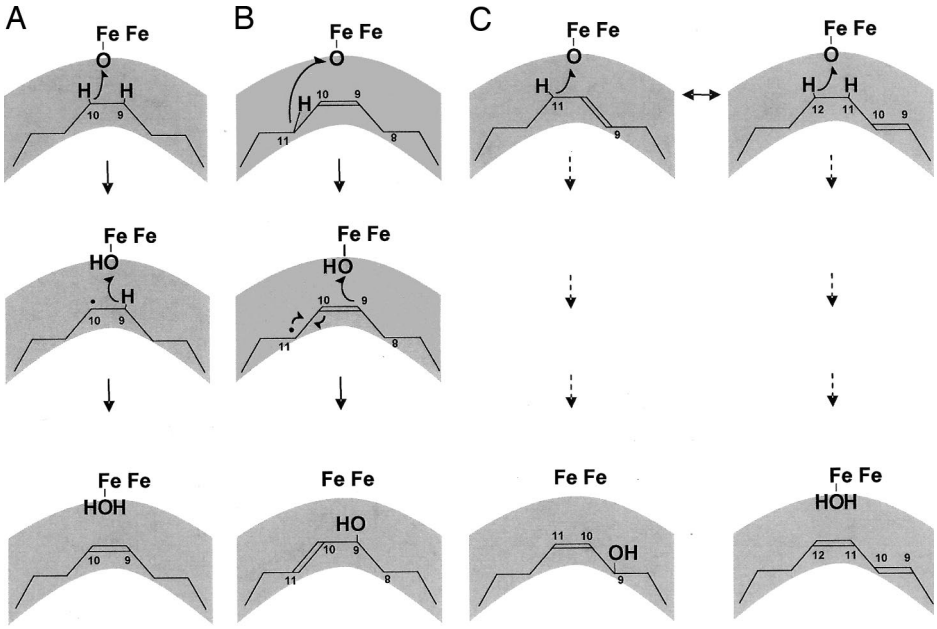

Fig. 4. Scheme illustrates the proposed substrate binding modes and reaction outcomes for various substrates with mutant desaturase. The mechanisms of (*Z*)-9-18:1 (*A*) and (*E*)-10-18:1-9-OH (*B*) formation are shown in the context of the bend in the desaturase substrate binding channel (gray) adjacent to the active site oxidant. (*C*) Postulated substrate binding modes of the nonnatural elaidyl substrate that leads to the formation of (*Z*)-10-18:1-9-OH and (*E*)-9-(*Z*)-11-18:2 are shown.

of the TMS derivatives of these standards with those of the reaction products reveal an excellent match for (*Z*)- or (*E*)-10-18:1-9-OH (compare Fig. 2*E* and *F* with Fig. 3 *F* and *G*); the mass spectrum of (*Z*)- and (*E*)-9-18:1-11-OH features an entirely different fragmentation pattern attributable to cleavage α to the O-TMS group between C-11 and C-12 (data not shown). This analysis leaves (*Z*)- and (*E*)-10-18:1-9-OH as the only possible candidates for the enzymatically generated allylic alcohols. Elucidation of the stereochemistry of these compounds was accomplished by a comparison of their GC elution times with those of our reference standards (Fig. 3 *B* and *C*). Spiking of the product mixture (Fig. 2*D*) with the (*Z*)-10-18:1-9-OH standard resulted in enhancement of the faster eluting peak labeled 3; the product peak spiked with the (*E*)-isomer is shown in Fig. 3*E*. Thus, the major (≈90%) product is (*E*)-10-18:1-9-OH, and the minor (≈10%) product is the corresponding (*Z*)-isomer.

Based on these results and the consensus mechanism for the WT enzyme (2) (Fig. 4*A*), we postulate that a hydrogen atom is abstracted at C-11 of oleyl-ACP by the oxidant; the resultant allylic radical is trapped regioselectively at C-9 by the iron-hydroxyl species (Fig. 4*B*). The curvature of the active site hinders rotation around the C-10, C-11 bond and yields primarily the (*E*)-product.

Elaidyl Substrate Is Converted to a Mixture of an Allylic Alcohol and a Diene. Our discovery that (*Z*)-9-18:1-ACP can act as a substrate for a soluble Δ9 desaturase variant is without precedent and offered a unique opportunity to probe the structural boundaries of a well characterized active site with stereochemically defined olefinic substrates. We asked whether (*E*)-9-18-ACP could act as a substrate with the mutant enzyme. Indeed, although a poorer substrate than the (*Z*) isomer (Table 2), (*E*)-9-18:1-ACP was converted primarily to a mixture of allylic alcohols and a diene component. The former consisted primarily of (*Z*)-10-18:1-9-OH along with minor amounts of (*E*)-10-18:1-9-OH (~10%) and coeluting (*E*)-9-18:1-11-OH (~3%) (determined by GC-MS spiking and single ion monitoring experiments using reference standards as described previously; data not shown). In addition to the allylic alcohols, a novel product produced in approximately equimolar ratio featured a molecular ion of *m*/*z* 294, suggesting that it is a dienoic C-18 fatty acid (Fig. 5*C*). Based on analysis of the mass fragmentation ladder of its pyrrolidine derivative (Fig. 5*D*) (21), the positions of the double bonds in the dienoic product were determined to be C-9 and C-11 (i.e., the product is a CLA).

To determine the stereochemistry of the double bonds, we compared the GC elution time of the product with those of 18:2 synthetic standards [(*E*)-9,(*Z*)-11/(*Z*)-9,(*Z*)-11 and (*Z*)-9,(*E*)-11/(*E*)-9,(*E*)-11], all of which had different retention times (Fig. 6 *B* and *D*). Spiking of the enzymic product with these standards allowed us to identify the dienoic product as the (*E*)-9,(*Z*)-11 isomer (Fig. 6*C*)—a product of (*Z*)-selective desaturation at C-11,C-12.

The Hydroxyl Oxygen Is Derived from O_2. The mechanistic pathway by which oleoyl-ACP is converted to the (*E*)-isomer of 9-OH 18:1Δ10 by the mutant acyl-ACP desaturase is reminiscent of that proposed for the biosynthesis of dimorphecolic acid from oleic acid (9)—a sequence that is thought to involve oxygenation of an allylic radical intermediate. Performing desaturase incubations in the presence of $^{18}O_2$ allowed us to establish the origin

Table 2. Kinetic parameters of the castor desaturase mutant T117R/G188L/D280K and wt enzyme

Enzyme	Substrate	k_{cat},* min^{-1}	K_M, μ M	Specificity factor k_{cat}/K_M, mol^{-1}·min^{-1}
mutant†	18:0	5.8‡ (0.50)	0.75 (0.14)	7.7
mutant	(*Z*)-9-18:1	0.18 (0.02)	1.60 (0.31)	0.11
wt	18:0	42.3 (1.6)	0.46 (0.05)	92.0

*k_{cat} is reported per diiron site.
†Mutant is T117R/G188L/D280K.
‡Mean with standard error in parentheses.

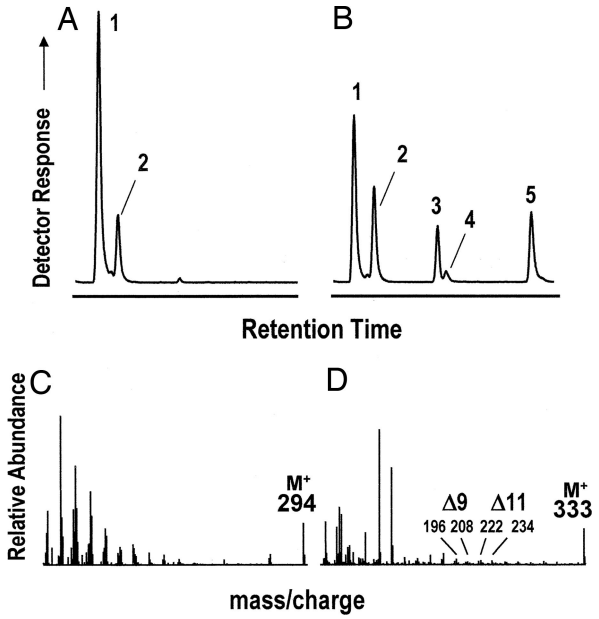

Fig. 5. Mutant desaturase converts (*E*)-9-18:1-ACP to hydroxy monoenes and CLA. Gas chromatographic separation of methyl esters following TMS derivatization of reaction mixtures containing (*E*)-9-18:1 substrate either before (*A*) or after (*B*) the addition of mutant desaturase enzyme. Fatty acid methyl esters: 1, (*E*)-9-18:1; 2, unidentified; 3, (*Z*)-10-18:1-9-OH; 4, (*E*)-10-18:1-9-OH; 5, 9-(*E*),11-(*Z*)-18:2 CLA. (C) Mass spectrum of methyl ester peak 5 is shown. (*D*) Mass spectrum of the pyrrolidine derivative of peak 5 is shown.

of oxygen atom in the allylic alcohol products. This approach is potentially capable of distinguishing between direct molecular oxygen-derived hydroxyl rebound to a radical intermediate or quenching of a carbocation by an active site water molecule (22). Thus, enzyme incubations were performed under an $^{18}O_2$ atmosphere for both (*Z*)- and (*E*)-9-18:1 substrates. The respective (*E*)- and (*Z*)-9-OH 18:1 product isomers were analyzed by MS (Table 3), and it was found that >98% of the oxygen in the hydroxyl groups in both products originated from molecular oxygen. The exclusive (within experimental error) incorporation of O_2-derived oxygen into the (*E*)- and (*Z*)-10-18:1-9-OH products is consistent with a mechanism involving hydroxyl rebound to an allylic radical (Fig. 4*B*). We recognize, however, that capture of an allylic carbocation by active site water derived from molecular oxygen remains a formal possibility.

The Shape of the Substrate Binding Cavity at the Active Site Influences Reaction Outcome. As described previously, the T117R/G188L/D280K mutant castor desaturase, like the WT enzyme, converts 18:0-ACP to (*Z*)-9-18:1-ACP. However, in contrast to the WT desaturase, the (*Z*)-9-18:1 moiety is further converted to mainly (*E*)-10-18:1-9-OH by the mutant. Notably, the 9-(*E*)-18:1 substrate is primarily converted to the 10-(*Z*)-9-OH product. We have yet to cocrystallize the substrates in the mutant enzyme successfully and are therefore not able to correlate substrate complexes with the observed products; however, the available desaturase crystal structures provide a useful context within which to rationalize the observed product stereochemistries. A key feature of the substrate binding cavity is its boomerang shape with a bend adjacent to the active site as predicted by Bloch (23) and revealed in subsequent crystal structures (12, 13). In the WT desaturase, the shape of the cavity (Fig. 1) forces the saturated substrate to adopt a quasi-eclipsed conformation at C-9 and C-10 with pro(*R*) hydrogens facing the diiron center (24). The available evidence (24–26) suggests that the site of initial oxidation

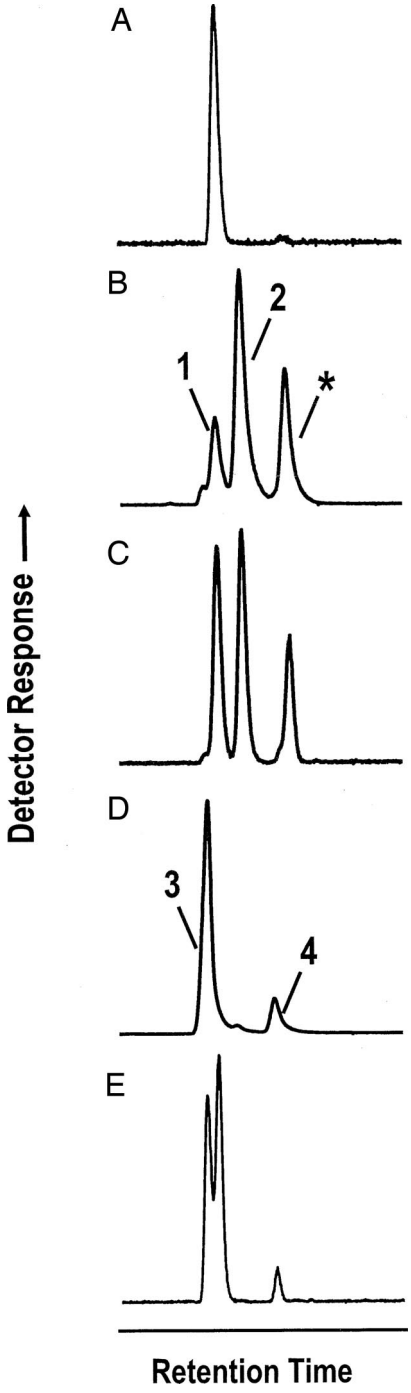

Fig. 6. (*A*) Gas chromatographic separation of methyl esters of: the mutant enzyme CLA product. (*B*) Standard mix of 1, (*E*)-9-(*Z*)-11-18:2, and 2, (*Z*)-9-(*Z*)-11-18:2. Asterisk indicates residual eneyne starting material (see the SI). (*C*) Combination of methyl esters from *A* and *B*. (*D*) Standard mix of 3, (*Z*)-9-(*E*)-11-18:2, and 4, (*E*)-9, (*E*)-11-18:2. (*E*) Combination of methyl esters from *A* and *D*.

may be at C-10 for WT enzyme (Fig. 4*A*). The T117R/G188L/D280K mutant enzyme allows the (*Z*)-9-18:1 substrate to bind in the active site because of changes remote from the diiron active site (Fig. 1) that might affect positioning of the pantetheine group linking the ACP to the fatty acid substrate (residue 280) or the methyl terminus of the fatty acyl portion of the substrate (residues 117 and 188). A possible binding mode for (*Z*)-9-18:1 is shown in Fig. 4*B* (compare with the binding of the natural 18:0-substrate shown in Fig. 4*A*). We envision hydrogen abstrac-

Table 3. Incorporation of ^{18}O into the hydroxyl group of the 10–18:1–9-OH product

	Product			
	(*Z*)-10-18:1-9-O TMS		(*E*)-10-18:1-9-O TMS	
Substrate	^{16}O	^{18}O	^{16}O	^{18}O
(*Z*)-9-18:1	1.6 (1.0)	98.4 (1.0)	2.0 (2.9)	98.0 (2.9)
(*E*)-9-18:1	0.3 (1.2)	99.7 (1.2)	nd	

Each incubation was carried out three times with >85% conversion; percentage of incorporation is reported as the average of the replicates; standard deviations are indicated in parentheses. Isotopic content was calculated by integration of mass spectral peaks at m/e 227/229, corrected for natural abundance isotopes. nd, not determined.

tion to proceed at the nearest available methylene group, namely C-11. The hydroxyl rebound occurs exclusively (>99.5%) at C-9 of the allylic radical along with the formation of a double bond between C-10 and C-11 that is principally in the (*E*)-configuration because of the curvature of the active site in this region. Thus, for this soluble desaturase mutant, like the previously reported case of membrane dimorphecolic acid-forming enzyme (9), hydrogen abstraction occurs at C-11 and the hydroxyl group is added at C-9. That the allylic 9-OH is the sole product implies that positioning of the (*Z*)-9-18:1 substrate must be precise; if it were not, we would perhaps expect to observe the formation of some 11-OH-9-ene product. Interestingly, 9-epoxy-stearate or the acetylenic compound, stearolic acid (9-octadecynoic acid) [i.e., products of oxidation observed in related enzymes (6)] are not detected (<0.5%), as judged by spiking experiments with authentic standards.

Further support for the hypothesis that the curvature of the active site adjacent to the diiron center is a primary determinant of reaction outcome was obtained from the incubation of (*E*)-9-18:1 with the mutant desaturase. According to our model, incomplete insertion of the acyl chain would be expected (Fig. 4*C*), such that collapse of the allylic radical intermediate would yield primarily a 9-hydroxylated product bearing a 10-(*Z*) double bond as is observed. With this substrate, a minor amount of 11-hydroxylated (≈3%) product is also formed by hydroxyl rebound to the site of initial hydrogen abstraction, and this compound bears a 9*E* double bond as anticipated. The concomitant formation of the conjugated diene suggests two possible binding modes of the (*E*)-9-18:1 substrate (Fig. 4*C*). The substrate complex favoring the introduction of the conjugated double bond is envisaged to arise from insertion of the fatty acyl chain slightly less deeply than that favoring allylic alcohol formation. In this mode, C-11 and C-12 are at the bend in the binding cavity, which dictates a quasi-eclipsed substrate conformation similar to that postulated for C-9 and C-10 of stearate in the WT enzyme, leading to the same configurational outcome [i.e., the (*Z*)-double bond] (Fig. 4 *A* and *C*). Precedence for this sort of regiochemical "error" product has been obtained with unnatural substrates (24, 27). The two binding-mode hypothesis and the stereochemistry of H-abstraction and hydroxyl rebound are the subject of current investigation.

The WT desaturase converts 18:0-substrate into 18:1 product, with no further oxidation. We have preliminary data that 18:1-ACP can inhibit the rate of desaturation, suggesting that it is capable of binding to the WT desaturase, but the absence of product formation suggests that the necessary conformational changes associated with redox gating are not triggered (28). How the three amino acid changes allow the binding and subsequent oxidation of 18:1-ACP in the mutant enzyme awaits the results of structural studies. Although the mutant castor desaturase described is a member of the soluble desaturase family, the sequential oxidation of stearoyl-ACP described herein is somewhat similar to the three consecutive oxidations of 16:0-CoA by a processionary moth pheromone gland membrane-bound desaturase (29).

Summary

The present study demonstrates the catalytic plasticity of diiron chemistry for a mutant soluble desaturase in which only three amino acids, remote from the active site, differ from that found in the WT sequence. In the mutant, the natural substrate 18:0-ACP is converted in a two-step oxidation reaction to mainly (*E*)-10-18:1-9-OH via a (*Z*)-9-18:1 intermediate. Incubation of a nonnatural substrate, (*E*)-9-18:1-ACP, resulted in the production of (*Z*)-10-18:1-9-OH and an (*E*)-9, (*Z*)-11 CLA isomer. Formation of these products can be rationalized in terms of distinct binding modes for the substrates that are conformationally constrained by curvature of the active site. That a triple mutant of the soluble desaturase expands the range of reaction outcome mimics that seen for the integral membrane class of desaturases and underscores the latent potential of O_2-dependent nonheme diiron enzymes to mediate a rich variety of functionalization chemistry. The data presented here provide novel and detailed mechanistic information on the factors governing the highly selective production of three unusual fatty acids.

Materials and Methods

Mutant Construction. A triple mutant T117R/G188L/D280K was engineered from the WT castor desaturase with the use of overlap extension PCR (30) to produce the D280K mutation with the use of the following pairs of primers, D280Kf gataatctttttaaacacttttcagctgttgcgc and D280Kr gcgcaacagctgaaaagtgtttaaaaagattatc, in conjunction with flanking pET9d primers. The fragment was introduced into the pET9d backbone after restriction with XbaI and EcoRI and cloning into the equivalent unique sites of pET9d. The T117R and G188L mutations were introduced by restriction of desaturase clone 5.2 (31) with NcoI and Acc65I and introduction of this fragment into the equivalent sites in the D280K mutant desaturase containing pET9d clone. Introduction of the T117R/G188L/D280K mutations was confirmed by sequencing.

Fatty Acid Analysis. Desaturase enzyme was generated by expression from a pET9d construct in *Escherichia coli* BL21(DE3) cells, followed by enrichment to >90% purity by 20CM cation exchange chromatography (Applied Biosystems). Fatty acid desaturase reactions (600 μl) were performed by incubation of the desaturase with 18:0-ACP and 18:1-ACP substrates in the presence of recombinant spinach ACP-I as previously described (32). Several deuterium-labeled substrates were obtained either from commercial sources (Cambridge Isotope Laboratories) or from the collection of Tulloch (20). Enzyme reactions were terminated by the addition of 1 ml of toluene. Fatty acid methyl esters (FAMEs) were prepared by the addition of 2 ml of 1% $NaOCH_3$ in methanol and incubation for 60 min at 50°C. The FAMES were extracted twice into 2 ml of hexane after acidification with 100 μl of glacial acetic acid. The 4 ml of hexane was evaporated to dryness under a stream of N_2, and resuspended in ~100 μl of hexane in preparation for GC analysis. For analysis of hydroxy fatty acids, the FAMEs were evaporated to dryness and resuspended in 100 μl of (*N,O-bis*[Trimethylsily]trifluoroacetamide plus trimethylchlorosilane (Supelco) for 45 min at 60°C to convert the hydroxy fatty acids to their trimethyl silyl derivatives. The FAMEs and their TMS derivatives were analyzed with the use of an HP5890 gas chromatograph-mass spectrometer (Hewlett-Packard) fitted with 60-m × 250-μm SP-2340 capillary columns (Supelco). The oven temperature was raised from 100°C to 160°C at a rate of 25°C min^{-1} and from 160°C to 240°C at a rate of 10°C min^{-1} with a flow rate of 1.1 ml/min^{-1}. Mass spectrometry was performed with an HP5973 mass selective detector (Hewlett-Packard). Authentic standards were prepared as described in the SI. For the ^{18}O experiments, oxygen was removed from the sample cell by repeated purging of the sample cell with O_2-free argon and vacuum with the use of a Schlenk line. Two samples were prepared, one containing desaturase enzyme, buffer, ferredoxin reduced nicotinamide adenine dinucleotide phosphate (NADPH)-positive reductase, and substrate, and the other containing ferredoxin and NADPH. Both samples were degassed by the application of 15 cycles of vacuum/argon; at that time; $^{18}O_2$ (98%) (Cambridge Isotope Laboratories) was introduced into the sample cell containing the desaturase and the degassed ferredoxin/NADPH was introduced to initiate the reaction. The

reaction was terminated by the introduction of toluene esterified and silylated as described previously.

ACKNOWLEDGMENTS. E.J.W. and J.S. thank the Office of Basic Energy Sciences of the U.S. Department of Energy, for financial support of this work. Support was also provided by Natural Sciences and Engineering Research Council (NSERC) (CGS-M postgraduate scholarship program to A.E.T., Grant OGP-2528 to P.H.B.). We thank Pat Covello for providing some of the deuterated compounds and Jodie Guy for structural comparisons of ivy and castor desaturase and for graphics assistance.

1. Millar AA, Smith MA, Kunst L (2000) All fatty acids are not equal: discrimination in plant membrane lipids. *Trends Plants Sci* 5:95–101.
2. Buist PH (2004) Fatty acid desaturases: selecting the dehydrogenation channel. *Nat Prod Rep* 21:249–262.
3. Fox BG, Shanklin J, Somerville C, Munck E (1993) Stearoyl-acyl carrier protein delta 9 desaturase from *Ricinus communis* is a diiron-oxo protein. *Proc Natl Acad Sci USA* 90:2486–2490.
4. Shanklin J, Achim C, Schmidt H, Fox BG, Munck E (1997) Mössbauer studies of alkane omega-hydroxylase: evidence for a diiron cluster in an integral-membrane enzyme. *Proc Natl Acad Sci USA* 94:2981–2986.
5. van de Loo FJ, Broun P, Turner S, Somerville C (1995) An oleate 12-hydroxylase from *Ricinus communis* L. is a fatty acyl desaturase homolog. *Proc Natl Acad Sci USA* 92:6743–6747.
6. Shanklin J, Cahoon EB (1998) Desaturation and related modifications of fatty acids. *Annu Rev Plant Physiol Plant Mol Biol* 49:611–641.
7. Lee M, *et al.* (1998) Identification of non-heme diiron proteins that catalyze triple bond and epoxy group formation. *Science* 280:915–918.
8. Cahoon EB, *et al.* (1999) Biosynthetic origin of conjugated double bonds: Production of fatty acid components of high-value drying oils in transgenic soybean embryos. *Proc Natl Acad Sci USA* 96:12935–12940.
9. Cahoon EB, Kinney AJ (2004) Dimorphecolic acid is synthesized by the coordinate activities of two divergent delta 12-oleic acid desaturases. *J Biol Chem* 12:12495–12502.
10. Broun P, Shanklin J, Whittle E, Somerville C (1998) Catalytic plasticity of fatty acid modification enzymes underlying chemical diversity of plant lipids. *Science* 282:1315–1317.
11. Broadwater JA, Whittle E, Shanklin J (2002) Desaturation and hydroxylation. Residues 148 and 324 of Arabidopsis FAD2, in addition to substrate chain length, exert a major influence in partitioning of catalytic specificity. *J Biol Chem* 277:15613–15620.
12. Lindqvist Y, Huang W, Schneider G, Shanklin J (1996) Crystal structure of a delta nine stearoyl-acyl carrier protein desaturase from castor seed and its relationship to other diiron proteins. *EMBO J* 15:4081–4092.
13. Moche M, Shanklin J, Ghoshal A, Lindqvist Y (2003) Azide and acetate complexes plus two iron-depleted crystal structures of the di-iron enzyme delta9 stearoyl-acyl carrier protein desaturase. Implications for oxygen activation and catalytic intermediates. *J Biol Chem* 278:25072–25080.
14. Guy JE, Whittle E, Kumaran D, Lindqvist Y, Shanklin J (2007) The crystal structure of the ivy Delta4-16:0-ACP desaturase reveals structural details of the oxidized active site and potential determinants of regioselectivity. *J Biol Chem* 282:19863–19871.
15. Dyer DH, Lyle KS, Rayment I, Fox BG (2005) X-ray structure of putative acyl-ACP desaturase DesA2 from Mycobacterium tuberculosis H37Rv. *Protein Sci* 14:1508–1517.
16. Bloomfield DK, Bloch K (1960) Formation of delta 9-unsaturated fatty acids. *J Biol Chem* 235:337–345.
17. Shanklin J, Somerville C (1991) Stearoyl-acyl-carrier-protein desaturase from higher plants is structurally unrelated to the animal and fungal homologs. *Proc Natl Acad Sci USA* 88:2510–2514.
18. Fox BG, Lyle KS, Rogge CE (2004) Reactions of the diiron enzyme stearoyl-acyl carrier protein desaturase. *Acc Chem Res* 37:421–429.
19. Sperling P, Ternes P, Zank TK, Heinz E (2003) The evolution of desaturases. *Prostaglandins, Leukotrienes and Essential Fatty Acids* 68:73–95.
20. Tulloch AP (1983) Synthesis, analysis and application of specifically deuterated lipids. *Prog Lipid Res* 22:235–256.
21. Andersson BA, Christie WW, Holman RT (1974) Mass spectrometric determination of positions of double bonds in polyunsaturated fatty acid pyrrolidines. *Lipids* 10:215–219.
22. Moe LA, Fox BG (2005) Oxygen-18 tracer studies of enzyme reactions with radical/cation diagnostic probes. *Biochem Biophys Res Commun* 338:240–249.
23. Bloch K (1969) Enzymatic synthesis of monounsaturated fatty acids. *Acc Chem Res* 2:193–202.
24. Behrouzian B, Savile CK, Dawson B, Buist PH, Shanklin J (2002) Exploring the hydroxylation-dehydrogenation connection: novel catalytic activity of castor stearoyl-ACP Delta(9) desaturase. *J Am Chem Soc* 124:3277–3283.
25. Rogge CE, Fox BG (2002) Desaturation, chain scission, and register-shift of oxygen-substituted fatty acids during reaction with stearoyl-ACP desaturase. *Biochemistry* 41:10141–10148.
26. White RD, Fox BG (2003) Chain cleavage and sulfoxidation of thiastearoyl-ACP upon reaction with stearoyl-ACP desaturase. *Biochemistry* 42:7828–7835.
27. Broadwater JA, Laundre BJ, Fox BG (2000) Desaturation of trans-octadecenoyl-acyl carrier protein by stearoyl-acyl carrier protein delta9 desaturase. *J Inorg Biochem* 78:7–14.
28. Reipa V, Shanklin J, Vilker V (2004) Substrate binding and the presence of ferredoxin affect the redox properties of the soluble plant Delta9-18:0-acyl carrier protein desaturase. *Chem Commun (Camb)* 21:2406–2407.
29. Serra M, Pina B, Abad JL, Camps F, Fabrias G (2007) A multifunctional desaturase involved in the biosynthesis of the processionary moth sex pheromone. *Proc Natl Acad Sci USA* 104:16444–16449.
30. Ho SN, Hunt HD, Horton RM, Pullen JK, Pease LR (1989) Site-directed mutagenesis by overlap extension using the polymerase chain reaction. *Gene* 77:51–59.
31. Whittle E, Shanklin J (2001) Engineering delta 9-16:0-acyl carrier protein (ACP) desaturase specificity based on combinatorial saturation mutagenesis and logical redesign of the castor delta 9–18:0-ACP desaturase. *J Biol Chem* 276:21500–21505.
32. Cahoon EB, Shanklin J (2000) Substrate-dependent mutant complementation to select fatty acid desaturase variants for metabolic engineering of plant seed oils. *Proc Natl Acad Sci USA* 97:12350–12355.